Computational and Structural Biotechnology Journal 20 (2022) 2134–2142

COMPUTATIONAL AND STRUCTURAL BIOTECHNOLOGY JOURNAL

journal homepage: www.elsevier.com/locate/csbj

Repurposing of thermally stable nucleic-acid aptamers for targeting tetrodotoxin (TTX)

Yuanyuan Li [a], Menghua Song [a], Ruihua Gao [b], Feng Lu [c], Jianping Liu [a,*], Qiang Huang [a,d,*]

[a] State Key Laboratory of Genetic Engineering, MOE Engineering Research Centre of Gene Technology, School of Life Sciences, Fudan University, Shanghai 200438, China
[b] State Key Laboratory of Molecular Engineering of Polymers, Department of Macromolecular Science, Fudan University, Shanghai 200438, China
[c] School of Pharmacy, Second Military Medical University, Shanghai 200433, China
[d] Multiscale Research Institute of Complex Systems, Fudan University, Shanghai 201203, China

ARTICLE INFO

Article history:
Received 11 February 2022
Received in revised form 23 April 2022
Accepted 23 April 2022
Available online 28 April 2022

Keywords:
Nucleic-acid aptamer
Tetrodotoxin
Drug repurposing
Molecular docking
Spontaneous binding simulation

ABSTRACT

Tetrodotoxin (TTX) is a lethal neurotoxin produced by the endosymbiotic bacteria in the gut of puffer fish. Currently, there is no effective and economical method to detect TTX, so it is very interesting to develop low-cost and high-sensitivity detection methods by using nucleic-acid aptamers as the recognition molecules. However, traditional SELEX screening of aptamers for targeting small molecules such as TTX is labor-intensive, and usually the success rate is low. Here, we employed a strategy of "repurposing old aptamers for new uses" to develop high-affinity aptamers for TTX. To this end, we first collected thermally stable DNA aptamers and predicted their affinities for TTX by molecular docking; then, we identified high-affinity candidates and verified them by microscale thermophoresis (MST) experiments. In this way, two thermally stable aptamers (Tv-51 and AI-57) were found to possess nanomolar affinities for TTX. Moreover, we performed spontaneous binding simulations to reveal their binding mechanisms to TTX and thereby identified the key bases for the binding. Guided by these, two variants (Tv-46 and AI-52) with higher affinities and specificities were subsequently engineered and confirmed by the MST experiments. So, this study not only provides potential recognition molecules for the technology developments of TTX detection, but also demonstrates an effective repurposing approach to the discovery of high-affinity aptamers for new target molecules.

1. Introduction

Tetrodotoxin (TTX) is an alkaloid marine toxin with low-molecular weight produced mainly by endosymbiotic bacteria in the gut of puffer fish (Fig. 1A) [1]. TTX is an inhibitor of sodium channel that could block the transport of sodium ions through the nerve and muscle cell membranes and thus leads to diarrhea and paralysis. Structural studies showed that the positively charged guanidine group in TTX interacts with the negatively charged carboxyl group located at the mouth of the sodium channel outside the plasma membrane of nerve and muscle cells [2,3]. And TTX is both water soluble and heat stable so cooking does not decrease its toxicity, but rather increases its toxic effect [4]. In recent years, people have suffered from the TTX damage due to the consumption of unclean puffer fish. It was reported that the toxicity of TTX is about 1000 times that of sodium cyanide, and intake of 1∼2 mg is sufficient to kill an adult [2,5]; moreover, currently no TTX antidote is available for clinical use [6]. The toxic symptoms of TTX after ingestion are dose-dependent. Mild dose toxic symptoms include tingling on the tongue and lips, followed by or concurrent with headache and vomiting; in severe conditions, this may progress to muscle weakness and ataxia; and in extreme cases death could occur due to respiratory and/or heart failure [6–8]. And the only treatment for TTX intoxication is observation and appropriate supportive care [5,7]. Therefore, it is important for us to detect TTX and to develop TTX antidotes in daily life.

In the past, various methods have been developed for detecting TTX, including mouse bioassay (MBA), enzyme-linked immunosorbent assay (ELISA), high performance liquid chromatography (HPLC), liquid chromatography-mass spectrometry (LC-MS) [9–11], etc. Among them, the sensitivity of MBA is low and its screening tests require living animals. And the screening tests of ELISA require the use of antibodies, and the toxicity of marine toxins

* Corresponding authors at: State Key Laboratory of Genetic Engineering, MOE Engineering Research Centre of Gene Technology, School of Life Sciences, Fudan University, Shanghai 200438, China (Q. Huang).
E-mail addresses: jpliu@fudan.edu.cn (J. Liu), huangqiang@fudan.edu.cn (Q. Huang).

https://doi.org/10.1016/j.csbj.2022.04.033
2001-0370/

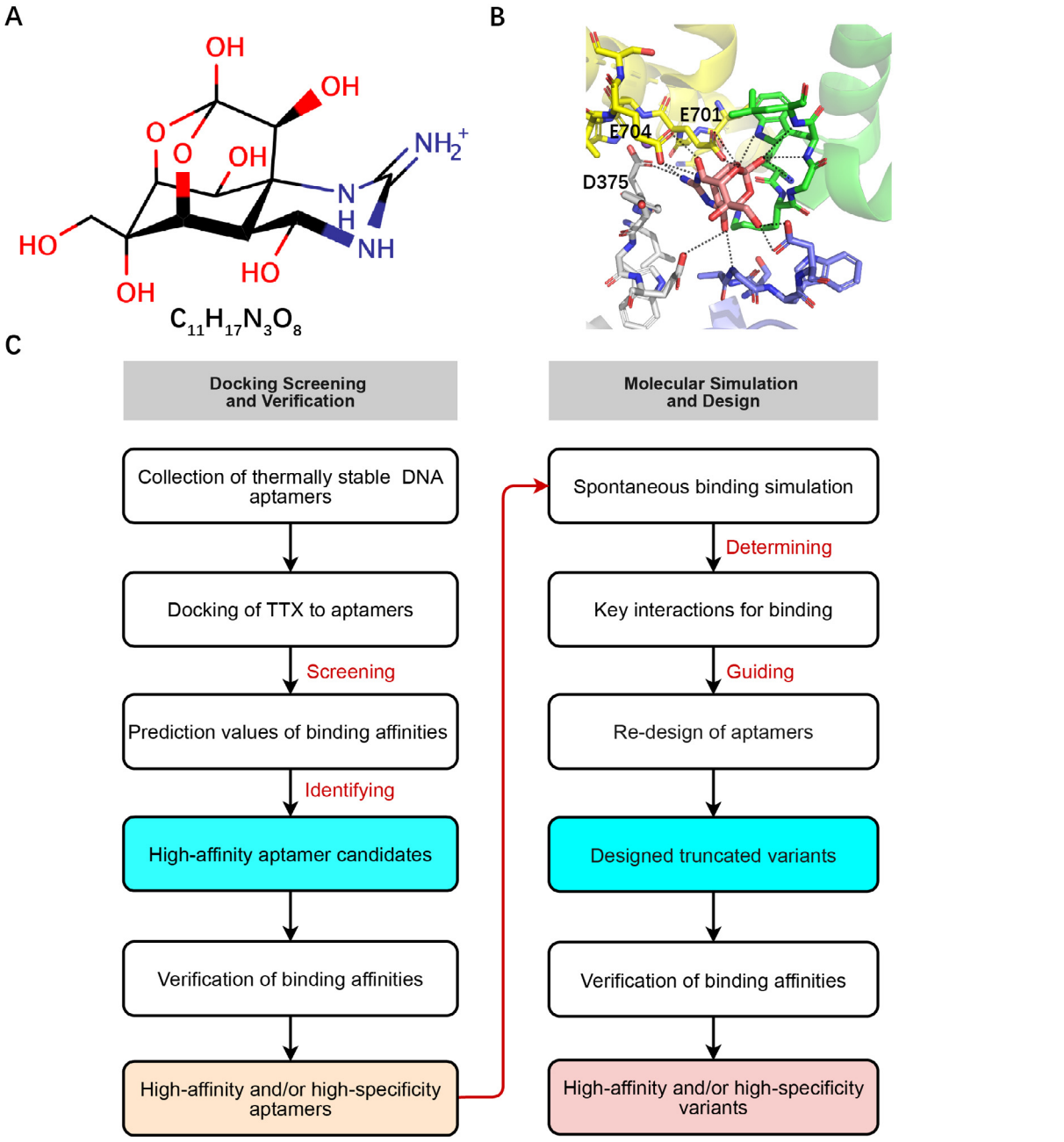

Fig. 1. Repurposing of old aptamers for targeting TTX. (A) Chemical structure of TTX. (B) Binding mode of TTX to the sodium channel. (C) Flowchart for discovering and engineering high-affinity and high-specificity aptamers of TTX by repurposing of thermally stable aptamers.

itself makes it difficult for organisms to produce antibodies, so the method is severely limited by the scarce supply of antibodies. Also, other detection methods have problems such as high cost, expensive equipment, sophisticated operation or high demand on technicians, etc. At the same time, there is no fast technology for on-site detection of water samples or toxic organisms [9,11]. Therefore, it remains very interesting to develop new rapid, sensitive and low-cost methods in the field of marine biotoxin detection such as TTX.

Recently, the rapid development and combination of aptamer screening technology and biosensor fabrication technology provide new approaches to the efficient detection of marine toxins such as TTX [12–15]. Aptamers are single-stranded oligonucleotides consisting of 20∼80 nucleotides and screened from a random library of 10^{12}∼10^{15} oligonucleotide sequences via SELEX (Systematic Evolution of Ligands by EXponential enrichment) [16–19]. Aptamers can fold into unique three-dimensional (3D) structures and bind to target molecules with high affinity and high specificity through shape complementarity, electrostatic interactions, van der Waals forces, and hydrogen bonds, so they are also known as "chemical antibodies" [20–22]. The equilibrium dissociation constants (K_d) of typical aptamers binding to their target molecules range from nM to μM [23]. And, aptamers have been used in assays and platforms that traditionally employed antibodies as analytical recognition elements [22,24,25]. Compared to antibodies, aptamers offer several unambiguous advantages due to their smaller size and nucleic-acid characteristics. For example, aptamers can easily penetrate into tissue barriers and are generally non-immunogenic or non-toxic *in vivo*, can eliminate the challenges associated with the limited availability of antibodies or the use of animals, and are cheap to synthesize or mass-produced and easy

to store or transport [13,21,25–27]. Therefore, the development of aptamers as analytical recognition elements has broad application prospects in the fields of toxin detection and antidote preparation. However, there are still many problems in the screening process of aptamers for TTX, such as long cycle, large sample consumption, low success rate and biased PCR amplification, which make it difficult to obtain aptamers with satisfactory affinity and specificity [14,28,29]. In addition, so far there are no reports about how TTX binds to aptamers, so it lacks rational methods to guide the optimal design of aptamers.

To address the above limitations, inspired by the drug discovery paradigm of "old drugs for new uses" and the TTX binding mode to sodium channel (Fig. 1B) [30], here we computationally screened existing aptamers for binding to TTX. We designated this strategy as "repurposing old aptamers for new uses", which mainly includes two steps, as illustrated in Fig. 1C. First, DNA aptamers with high thermal stability (T_m > 50°C) were collected, and the candidate aptamers for TTX were screened by molecular docking; then the binding abilities of the candidate aptamers were verified by microscale thermophoresis (MST) experiments. Secondly, spontaneous binding processes of TTX to the aptamers were studied by unbiased molecular dynamics (MD) simulation to confirm the binding mode revealed in the molecular docking; and according to the structural information obtained in the simulations, variants were then engineered for stronger binding affinity or/and specificity. In this strategy, we found that two old aptamers (Tv-51 and AI-57) possess high binding affinities for TTX. Based on them, two variants (Tv-46 and AI-52) were further engineered for specifically targeting TTX. To the best of our knowledge, this is the first example to develop TTX aptamers by employing existing aptamers with good thermal stability.

2. Materials and methods

2.1. Structural prediction of aptamers

We predicted the secondary structure of a given DNA aptamer via the *RNAstructure* web server at https://rna.urmc.rochester.edu/RNAstructureWeb/Servers/Predict1/Predict1.html [31]. With the predicted secondary structure, we used the *rna_assembly* module in the Rosetta software to predict the 3D structure of the given aptamer [32–34]. First, the sequence and secondary structure files of the aptamer were prepared: "T" was changed to "U" in the FASTA file. Then, ideal A-type helix was created for each helical segment longer than two base pairs. The remaining bases were modeled by using FARNA (Fragment Assemble of RNA with full atom refinement) to generate more than 4000 possible models. Finally, the models of separately built motifs and helices were assembled and optimized through the FARNA Monte Carlo procedure and the 3D structure with the lowest energy was obtained.

2.2. Molecular docking

As in our previous work [35–37], we employed the AutoDock4.2 [38–40] package to perform the semiflexible global docking of TTX to aptamers. This package mainly contains two programs called AutoGrid and AutoDock. Many studies in the past decade have confirmed its ability to correctly predict the binding affinities of the ligands to receptors, including our study. AutoDock4.2 evaluates the binding free energy of docking conformations on the basis of a semiempirical free energy force field [40,41] by two steps: The first step evaluates the intramolecular energetics ($\Delta G_{intramol}$) of the transition from these unbound states to the conformation that the ligand or receptor will adopt in the bound complex; the second step evaluates the intermolecular energetics ($\Delta G_{intermol}$) of combining the ligand and receptor in their bound conformations. And the binding free energy and K_d are:

$$\begin{aligned}\Delta G_{bound} &= \Delta G_{intramol} + \Delta G_{intermol} \\ &= \left(\left(V^{T-T}_{bound} + V^{A-A}_{bound}\right) - \left(V^{T-T}_{unbound} + V^{A-A}_{unbound}\right)\right) \\ &\quad + \left(V^{T-A}_{bound} - V^{T-A}_{unbound} + \Delta S_{conf}\right)\end{aligned} \tag{1}$$

$$K_d = exp\left(\frac{\Delta G_{bound}}{RT}\right) \tag{2}$$

In Eq. (1), T represents the flexible ligand "TTX" and A represents the rigid receptor "aptamer"; V is the potential function and ΔS_{conf} is the conformational entropy lost upon binding. In Eq. (2), R is the ideal gas constant of 8.314 J $mol^{-1}K^{-1}$ and T is the room temperature of 298.15 K.

In addition, AutoDock4.2 calculates the intermolecular energy (including hydrogen bonds, van der Waals forces, desolvation and electrostatic interactions) by a parametrized grid in AutoGrid program; searches the conformation and optimizes the energy by Lamarckian genetic algorithm (LGA) in AutoDock program. And Python programs in AutoDockTools [40] were used to calculate the parameters of the aptamers and TTX according to standard procedures.

2.3. Spontaneous binding simulation of TTX to aptamers

Similar to our previous studies [35–37] we employed GROMACS (Ver. 5.1.4) [42] to perform the spontaneous binding simulations with the AMBER99bsc1 force fields and SPC water model [43]. TTX was prepared by Antechamber with the General Amber Force Field (GAFF) [44]. The topology and coordinate files of TTX were generated by the LEaP program in AmberTools 17 and then were converted to GROMACS-compatible files by ACPYPE [45]. For each system, the aptamer was placed in the center of a water box, with a distance from its surface to the box boundaries >15 Å. TTX was randomly placed at least 15 Å away from the aptamer. Na^+ and Cl^- ions were placed by random replacement of the water molecules for neutralizing the system and mimicking an ionic concentration of 150 mM. Periodic boundary conditions were used in the simulations; a cut-off distance of 14 Å was used for the short-distance electrostatic and van der Waals forces, and the Particle-Mesh-Ewald (PME) algorithm was used to calculate the long-distance electrostatic interactions [46]. The LINCS algorithm was used to constrain all bonds in the systems, and thereby a time step of 2.0 fs was used [47]. The velocity rescaling and Berendsen methods were used to control the system temperature and pressure at 300 K and 1.013 bar, respectively [48,49]. Each independent simulation was performed for at least 500 ns.

2.4. Structural analysis

In the MD trajectory analyses, root-mean-square deviation (RMSD) was employed to evaluate the conformational differences of the snapshot structures of the aptamers by using the starting conformation as the reference; and root-mean-square-fluctuation (RMSF) was employed to evaluate the flexibility of the aptamer bases. The RMSDs and RMSFs were computed via GROMACS tools. In addition, the hydrogen bond (HB) contacts and van der Waals (vdW) forces between a ligand (TTX) and the given receptor (aptamer) were estimated using the related GROMACS programs and homemade nearest-contact scripts of TTX atoms and aptamer bases.

2.5. Microscale thermophoresis (MST)

The MST experiments of TTX and aptamers were performed on Monolith NT.115 (NanoTemper Technologies, Germany), and the binding affinity was characterized by the equilibrium dissociation constant (K_d) [50]. Before the MST experiments, the aptamers labeled with 6-FAM fluorescence were dissolved in the buffer (50 mM Tris-HCl, pH 7.5, 150 mM NaCl, 2 mM $MgCl_2$) to 100 nM, heated at 95°C for 10 min, then quenched in ice bath for 5 min, and finally placed at room temperature for 5 min to complete the pretreatment of aptamers. Then, 16 groups of TTX solution were diluted with 0.1% Tween-20 buffer at a ratio of 1:1 (the highest concentration was 4000 nM), and then the equal volumes of aptamers were added to the solution. Finally, in the binding buffer (containing 0.05% Tween-20), the concentration range of TTX was from 0.061 to 2000 nM, and the constant concentration of aptamers was 50 nM. The appropriate LED power was chosen to control the fluorescence value between 800 and 1500. The MST power was set to 40%, the thermophoresis time (t) was 30 s, and the experimental temperature (T) was 25°C. At least three independent experiments were repeated and then the data were imported into MO. Affinity analysis software of NanoTemper to calculate the K_d value of TTX binding to the aptamers.

2.6. Circular dichroism (CD)

The CD spectra were recorded using a Chirascan spectrometer (Applied Photophysics, Ltd.) at 25°C [51]. The 5 μM aptamers and its mixture with 10 μM TTX were prepared. Note that the aptamers should be pretreated in the same way as MST. The data were collected from 200 nm to 360 nm in a 1 mm path-length quartz cuvette at a scanning rate of 120 nm min^{-1} and presented as an average of three successive scans finally. Note that the data were buffer subtracted and normalized to provide the molar ellipticity values.

2.7. Chemical agents

All DNA aptamers were purchased from Sangon Biotech Co., Ltd (Shanghai, China). The sequences of aptamers are listed in Supplementary Table S1. The toxins TTX, GTX, OA and NOD were purchased from Puhuashi Technology Development Co., Ltd (Beijing, China). Tris, NaCl, $MgCl_2$ and Tween-20 were purchased from Sangon Biotech Co., Ltd (Shanghai, China). NaOH and HCl were purchased from Sinopharm Chemical Reagent Co., Ltd (Shanghai, China). All chemical reagents were of analytical grade and used without further purification.

3. Results

3.1. Docking screening of candidate aptamers for TTX

To understand the characteristics of the aptamers that potentially bind to TTX, we analyzed the binding mode of TTX to the 3D structure of the sodium channel [30]. As seen in Fig. 1A, TTX contains six hydroxyl groups and one guanidine group, and was predicted to be positively charged at neutral or weakly basic pH by the MarvinSketch software. Corresponding to this (Fig. 1B), the sodium channel is geometrically matched to the shape of TTX and is rich in negatively charged residues. As seen, TTX occupies the entrance to the sodium channel through an extensive network of electrostatic interactions and binds to the amino acids around the entrance via polar interactions. Particularly, TTX forms multiple hydrogen bonds and salt bridges with Asp375, Glu701 and Glu704 (the Na^+ binding site, known as "DEE" sites) at the entrance, and thus tightly blocks the sodium channel. Such a binding mode inspired us that the phosphate backbones of nucleic-acid aptamers are negatively charged, so they might act as binding sites for TTX. If a given aptamer possesses a pocket that could accommodate TTX and has the bases that could interact with TTX, this aptamer is a potential binder of TTX.

To collect existing aptamers that potentially bind to TTX, we focused on their stability and shape complementarity with TTX. We collected DNA aptamers from previous publications and removed the double-chain hybrid sequences. Then, we calculated their T_m values with the sangon web server (https://www.sangon.com/baseCalculator) and removed the aptamers with a T_m value < 50°C. Next, TTX was moved into the cavity or groove of the aptamer 3D structures by PyMOL to inspect if the aptamers could contain TTX in space, and those that could not match the TTX geometry were excluded. In this step, the aptamers without experimental 3D structures were predicted using the methods in Subsec. 2.1. Eventually, 12 thermally stable aptamers were obtained for the repurposing, as listed in Table S2. Except for two aptamers (Tv-51 and AI-57), other 10 aptamers already have experimental structures. So, the 2D and 3D structures of Tv-51 and AI-57 were predicted with the methods in Subsec. 2.1 (Fig. 2, Fig. S1). Notably, the T_m values of both aptamers are greater than 80°C, indicating that they are thermally stable. Indeed, their original molecules (named anti-vWF and anti-IFNγ) [52] are DNA aptamers with 2 unnatural bases and 2 mini-hairpins (Fig. S2). To be able to synthesize, we replaced the unnatural bases with T and A, and obtained the aptamers designated as Tv-51 and AI-57, respectively. Compared to the original forms, Tv-51 and AI-57 retain thermally stable DNA mini-hairpins (1 and 2 mini-hairpins, respectively) and generate new stem-loop and cavity structures, which was considered to provide favorable binding interactions with TTX.

To rapidly assess the binding abilities of the collected aptamers for TTX, we performed global molecular docking by using TTX as the ligand and the aptamers as the receptors. The initial structure of TTX was taken from PDB ID 6A95. Docking results showed that the calculated K_d values of TTX to several aptamers are relatively low, especially those of Tv-51 and AI-57 are much lower (Table S2). Since the 3D structures of Tv-51 and AI-57 used in the docking were the predicted structures, to ensure the docking reliable, we decided to perform the second round of docking by using the MD refined structures (Fig. S3). Then, we selected these two aptamers and the following three aptamers with experimental structures to perform the second round of docking. As shown in Table 1, the calculated K_d values of the 5 aptamers in complex with TTX are all at the magnitude of nanomoles (nM). Again, those of Tv-51 and AI-57 are the lowest. In addition, the docking results using the MD refined structures were slightly different from the initial results, implying that the refinements of the predicted aptamer structures by MD simulations are necessary. Furthermore, MD simulations were also performed for the three aptamers with experimental structures, in order to confirm the reliability of our methods. As shown in Fig. S4, the small RMSD fluctuations with the simulation time indicated that the aptamer structures in the simulations are stable with respect to the initial structures (i.e., the experimental structures). Therefore, the MD structures are very similar to the experimental structures. Taken together, the 5 aptamers with the highest calculated affinities were eventually chosen as the candidates for the following experimental tests.

3.2. Binding affinity measurements of TTX-binding aptamers

To verify the binding affinities of the 5 candidate aptamers for TTX, we used MST experiments to determine their K_d values. Results showed that Tv-51 possesses the highest binding affinity

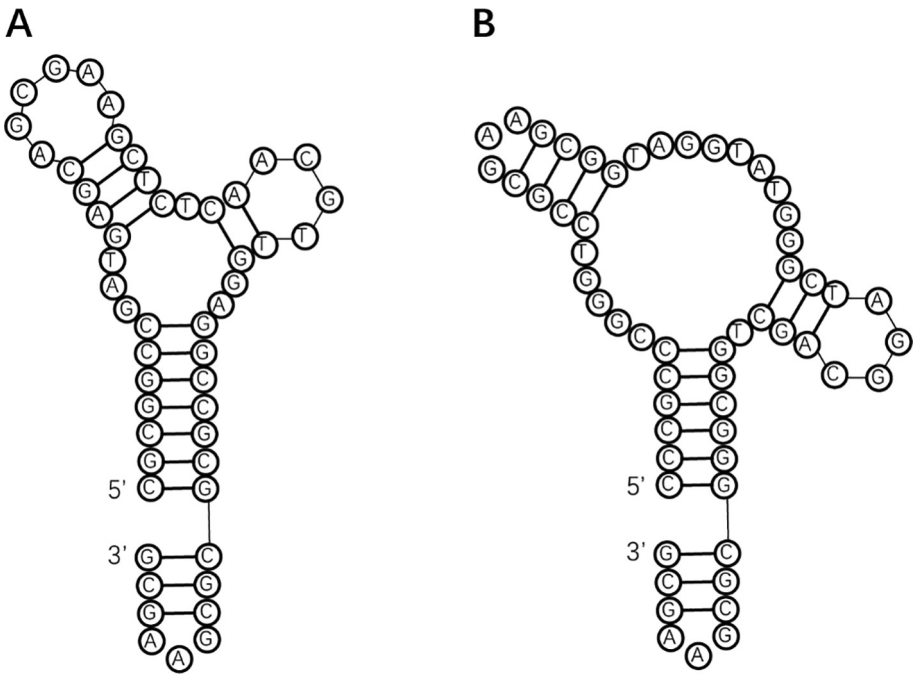

Fig. 2. Secondary structures predicted by the *RNAstructure* web server. (A) Tv-51. (B) AI-57.

Table 1
Equilibrium dissociation constants of TTX with aptamers by molecular docking and MST.

Name or PDB ID	ΔG (kcal/mol)	AutoDock Kd (nM)	MST Kd (nM)	Predicted Tm (°C)
Tv-51	−11.82	2.16	14.92 ± 0.19	83.24
AI-57	−10.61	16.61	28.34 ± 0.13	87.13
2L5K	−10.50	19.99	No binding	55.31
2IDN	−10.10	39.60	No binding	50.40
2ARG	−9.99	47.74	100.91 ± 0.34	68.69

* T_m was calculated via the sangon web server (https://www.sangon.com/baseCalculator).

and its K_d is 14.92 ± 0.19 nM; those of AI-57 and 2ARG are 28.34 ± 0.13 nM and 100.91 ± 0.34 nM, respectively (Fig. 3A, Table 1). So, the K_d values of Tv-51 and AI-57 are less than 50 nM. In contrast, the MST results indicated that the other two candidate aptamers (2L5K and 2IDN) could not bind to TTX. This might be attributed to the poor shape complementarity between the aptamers and TTX. For example, the docking showed that the binding sites are close to the 3′ and 5′ ends; however, the MD simulations showed that the aptamer conformations near those flexible ends changed significantly (Fig. S5).

To test their binding specificities for TTX, we determined the binding affinities of Tv-51 and AI-57 for other 3 marine toxins. These 3 toxins are polyether okadaic acid (OA), polypeptide nodularin (NOD), and gonyautoxin (GTX) which is also an alkaloid like TTX (Fig. S6) [53]. MST results showed that both the aptamers do not bind to NOD; the K_d values of Tv-51 and AT-57 to OA are 135.56 ± 0.43 and 56.74 ± 0.43 nM, respectively; and the K_d values of Tv-51 and AI-57 to GTX are 71.61 ± 0.36 and 308.41 ± 0.55 nM, respectively (Fig. 3B, 3C, Table 2). Thus, the binding affinities of the aptamers to the other 3 toxins are lower than those for TTX, suggesting that Tv-51 and AI-57 are more specific for TTX.

Finally, we also investigated the conformational changes of the aptamers (AI-57 and Tv-51) upon the TTX binding by CD spectra. CD results showed that the aptamer conformations do not change in the presence of TTX (Fig. 3D, Fig S7). The positive peak at 278 nm and the negative peak at 249 nm represent the formation of B-form duplex resulted from the stem-loop structures of Tv-51. Similarly, the positive peak at 280 nm and the negative peak at 254 nm reflect the formation of B-form duplex resulted from the stem-loop structures of AI-57. Therefore, the aptamer conformations are stable in the absence and presence of TTX, and both aptamers have the stem-loop structures as predicted.

3.3. Atomistic modelling of TTX binding to Tv-51 and AI-57

According to the docking poses of TTX to Tv-51 and AI-57, we found that TTX is bound to the grooves formed by the stem-loops of the aptamers (Fig. S8). This indicated that these stem-loops provide potential binding sites for TTX. To confirm the binding modes, we performed spontaneous binding simulations for the Tv-51:TTX and AI-57:TTX systems, as in previous studies [36,37]. Our MD simulations successfully captured the binding processes of TTX to the aptamers. In the simulations, TTX was first attracted to the phosphate backbone of the aptamers and then bound to the aptamers; after that, the aptamers continuously adjusted its binding positions until TTX was tightly complexed with the grooves formed by stem-loops (Movies S1 and S2). Very significantly, the binding sites revealed by the spontaneous binding simulations are consistent with those in molecular docking, strongly suggesting that TTX binds to the minor grooves of the stem-loops in the two aptamers.

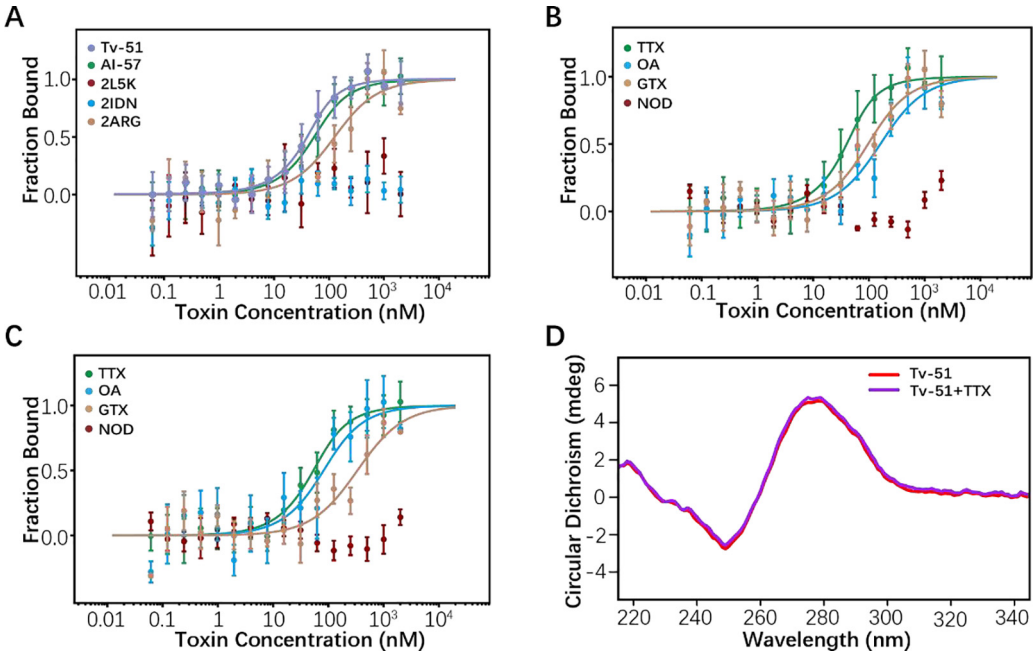

Fig. 3. Binding affinity measurements of TTX to aptamers. (A) MST experiments for candidate aptamers. (B) Binding specificity of TTX to Tv-51. (C) Binding specificity of TTX to AI-57. (D) CD spectra of Tv-51 (5 μM) and its mixture with TTX (10 μM).

Table 2
Equilibrium dissociation constants of marine toxins to the aptamers by MST.

Aptamer:Toxin Complex	MST Kd (nM)	Variant:Toxin Complex	MST Kd (nM)
Tv-51:TTX	14.92 ± 0.19	Tv-46:TTX	13.52 ± 0.18
Tv-51:NOD	No binding	Tv-46:NOD	No binding
Tv-51:OA	135.56 ± 0.43	Tv-46:OA	254.30 ± 0.28
Tv-51:GTX	71.61 ± 0.36	Tv-46:GTX	645.05 ± 0.35
AI-57:TTX	28.34 ± 0.13	AI-52:TTX	6.61 ± 0.22
AI-57:NOD	No binding	AI-52:NOD	No binding
AI-57:OA	56.74 ± 0.43	AI-52:OA	431.67 ± 0.32
AI-57:GTX	308.41 ± 0.55	AI-57:GTX	722.61 ± 0.33

In the Tv-51:TTX system, TTX was first attracted by other stem-loop, and then entered the target stem-loop at about 349 ns (Movie S1). This process implied that Tv-51 has bases that may prevent TTX from entering the target binding site. Moreover, the RMSD values with the simulation time showed that the system has been equilibrated during 350–750 ns, indicating that TTX has been stably bound to Tv-51 (Fig. 4A). In the AI-57:TTX system, TTX was quickly attracted by the target stem-loop, and there was almost no base contact with the intermediate cavity or other parts, suggesting that AI-57 has redundant bases that could be truncated (Movie S2). Furthermore, when the simulation time exceeded about 545 ns, the AI-57:TTX complex approached a stable binding state (Fig. S9). Therefore, we confirmed that TTX is stably bound to the grooves formed by the new stem-loops of aptamers, and identified other redundant bases, which provides a direction for the following optimization design.

To reveal the binding mode of TTX to the aptamers at the atomic level, we determined the key binding bases by calculating the average vdW forces and H-bonds for each base to TTX in the simulation process (Movies S1 and S2). To characterize the vdW forces, we first calculated all the pairwise distances between the TTX atoms and aptamer bases for each MD frame in the periods of the stable binding. Then, we identified the base with the smallest distance to TTX atoms in each MD frame, and designated that base as the nearest-contact base. Finally, we calculated the probabilities of the aptamer bases as the nearest-contact base of TTX in the simulations. The results showed that in the Tv-51:TTX system, the probabilities of C26 and G33 as the nearest-contact base are 0.32 and 0.34, respectively; those of A9 and A28 are 0.15 and 0.10, respectively; and the others are less than 0.05 (Fig. 4B). To characterize the H-bonds, we calculated the average numbers of H-bonds between TTX and the aptamer bases in the simulations. As shown in Fig. 4B, the average H-bond numbers formed by TTX with A9, C26 and G33 are 1.62, 1.50 and 1.06, respectively; those of A28 and G34 are 0.74 and 0.69, respectively; and the others are less than 0.50. Therefore, TTX mainly interacts with A9, C26, A28, G33 and G34 of Tv-51. In the AI-57:TTX system, the probabilities of C33 and T34 as the nearest-contact base are 0.67 and 0.26, respectively; and the others are less than 0.05. The average H-bond numbers formed by TTX with C33, T34 and A35 are 1.25, 0.61 and 1.32, respectively; and the remaining H-bonds are less than 0.50 (Fig. 4C). Therefore, TTX mainly interacts with C33, T34 and A35 of AI-57.

3.4. Re-design of AI-57 and Tv-51

As mentioned, the spontaneous binding simulation and interaction calculation have shown that TTX is unbound to the intermediate cavity of AI-57, and even the bases in the cavity do not contact with TTX. This is probably because the cavity is too large to match the TTX geometry. And it is natural to assume that the cavity might contain redundant bases that have no significant contribution to the TTX binding. Therefore, those bases in the cavity of AI-57 were gradually removed, and the secondary structures and T_m values of the aptamer variants were predicted. In this way, the bases originally at positions 7, 26 and 29–31 were removed, and T at position 42 was mutated to A to obtain a variant AI-52 (T_m = 85.67°C) (Fig. S10). Also, we predicted the 3D structure of AI-52 (Fig. S11) and performed molecular docking for it. The docking K_d value of TTX to AI-52 is 3.78 nM, and less than that of AI-57 (K_d = 16.61 nM). By comparing the 3D structure of AI-52 with that of AI-57, we found that the distance between the original binding site and the intermediate cavity skeletons of AI-52 is reduced. And molecular

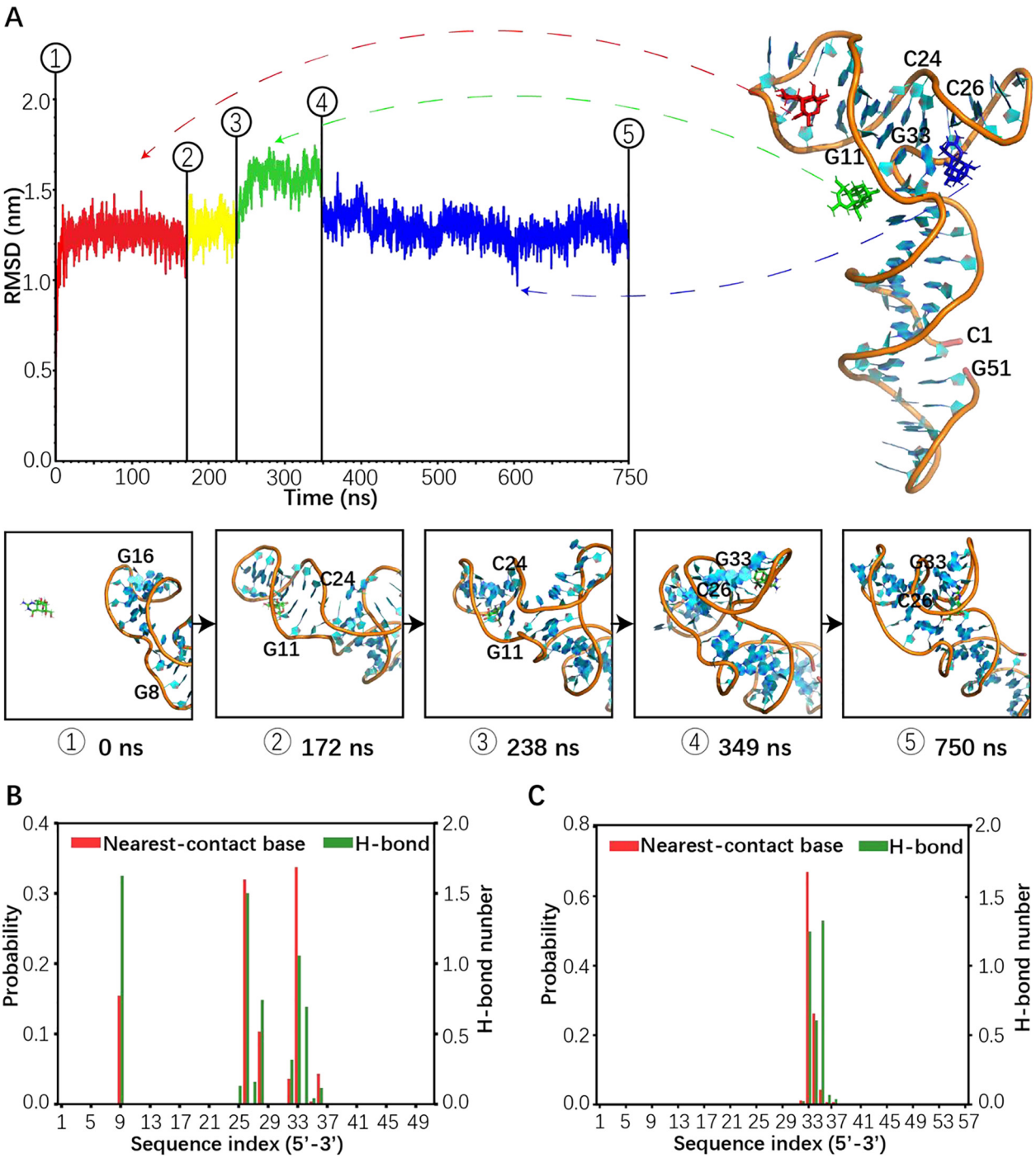

Fig. 4. Spontaneous association of TTX with Tv-51 and the complex structure of Tv-51:TTX. (A) Time-dependent RMSDs of the Tv-51:TTX complex, and corresponding binding positions of TTX on Tv-51. The position of TTX at a given time was obtained by aligning the corresponding snapshot with the last frame of the simulations. Five representative association changes are given in the panels below. Corresponding movie showing the spontaneous association process is presented in Supplementary Movie S1. (B) and (C) Residue-based interactions: the probabilities of aptamer bases as the nearest-contact bases of TTX (in red); the average H-bond numbers between TTX and the bases (in green). (For interpretation of the references to colour in this figure legend, the reader is referred to the web version of this article.)

docking showed that TTX binds to the new cavity surrounded by these phosphate skeletons (Fig. 5A). It appears that the removal of these redundant bases provides a better binding site for TTX and thereby enhances the binding affinity.

The spontaneous binding simulation and interaction calculation of Tv-51 have shown that the bases at positions 11–24 hinder the binding of TTX. Therefore, it is natural to engineer variants by deleting those bases gradually. A truncated variant Tv-46 (T_m = 84.19°C) was then engineered by removing the bases originally at positions 12, 15–17 and 23, respectively (Figs. S12 and S13). Compared to Tv-51 (containing 1 mini-hairpin), Tv-46 has 2 mini-hairpins, which could further stabilize the aptamer structure. Similarly, we performed molecular docking for Tv-46 and TTX. The results showed that TTX binds to the intermediate cavity of Tv-46 (Fig. S14A), and the K_d value is 2.07 nM, which is close to the calculated value of Tv-51 (K_d = 2.16 nM). Thus, removing these bases has no significant effects on the affinity. Note that the binding sites of both the truncated aptamers change from the stem-loops to the

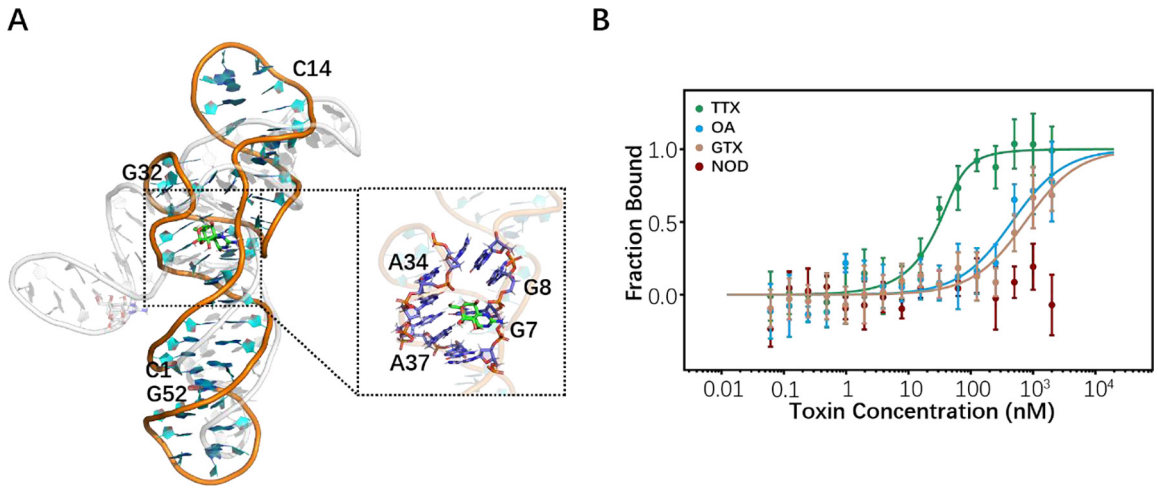

Fig. 5. Re-design of AI-57 for the optimized variant (AI-52). (A) Molecular docking of TTX to AI-52, where AI-52 (cyan) is aligned to AI-57 (white). (B) Binding specificity of TTX to AI-52. (For interpretation of the references to colour in this figure legend, the reader is referred to the web version of this article.)

intermediate cavities, which indicated that removing those bases not only shortens the distance between the stem-loops and the intermediate pocket backbones, but also reduces the flexibility of the cavities, and thereby forms the binding pockets that match the shape of TTX.

Finally, we detected the binding affinities and specificities of the aptamer variants (Fig. 5B, Fig. S14B, Table 2). The K_d values of AI-52 and Tv-46 to TTX are 6.61 ± 0.22 nM and 13.52 ± 0.18 nM, respectively; and the variants do not bind to NOD. The K_d values of AI-52 to OA and GXT are 431.67 ± 0.32 nM and 722.61 ± 0.33 nM, respectively, higher than those of AI-57. Compared to AI-57, the truncated variant AI-52 has higher affinity and specificity for TTX. The K_d values of Tv-46 to OA and GXT are 254.30 ± 0.28 nM and 645.05 ± 0.35 nM, respectively, higher than those of Tv-51. Therefore, the affinities of Tv-46 and Tv-51 for TTX are similar but the specificity of Tv-46 is stronger. Taken together, by the approach of "repurposing old aptamers for new uses", 4 new TTX aptamers (AI-57, AI-52, Tv-51 and Tv-46) were discovered or engineered.

4. Discussion and conclusion

In this study, we have successfully employed the approach of "repurposing old aptamers for new uses" to develop 4 new high-affinity aptamers for TTX. We collected old, thermally stable DNA aptamers and then predicted their affinities of binding to TTX by molecular docking. Verified by the MST experiments, two thermally stable aptamers (Tv-51 and AI-57) were found to possess nanomolar affinities for TTX. Then, we performed spontaneous binding simulations to identify their key bases for the TTX binding, and thereby engineered two aptamer variants (Tv-46 and AI-52) with higher affinities and specificities, mainly by removing redundant nucleotides in the old aptamers. So, this study demonstrates that "repurposing old aptamers for new uses" is a very promising approach to the discovery of high-affinity aptamers for targeting small molecules, and the rational engineering from the old aptamers by molecular modeling could obtain new aptamers with higher affinities and specificities.

As known, although the traditional SELEX method for the nucleic-acid aptamers has been relatively mature, its screening is still complicated and low-efficiency, and often fails to find aptamers with the same binding affinity as antibodies [17]. Similarly, improved screening methods, like counter SELEX, capillary electrophoresis SELEX and microfluidic SELEX, also have unsolved issues, such as lack of versatility, complex operation and high-difficulty technology etc. [20,54]. Therefore, it is still necessary to develop new discovery and design methods of aptamers. Inspired by the approach of "old drugs for new uses", in this study we developed the method of "repurposing old aptamers for new uses" for finding new TTX aptamers from the old, thermally stable aptamers. With it, we have obtained the new DNA aptamers of which affinities are higher than that of the best SELEX aptamer TTX-07 (K_d = 44.12 ± 15.38 nM, determined by fluorescence assay) [55]. These high-affinity aptamers could be used as the recognition components of biosensors for the detection of TTX, or as the targeting molecules on the nanoparticle surfaces in the nanoparticle-aptamer coupling technology for disease treatments [56].

In addition, the structures of the aptamer-TTX complexes are usually difficult to be determined by experimental methods, such as X-ray crystallographic and NMR methods, etc. In this study, we used molecular modeling methods to predict the binding processes and modes of TTX to the aptamers. The molecular docking may quickly calculate the binding affinities of TTX to the aptamers, and thus screen the high-affinity aptamers from many candidates. And the spontaneous binding simulations could identify the key bases of the aptamers for the TTX binding, thereby accurately guide the optimization of aptamers. Therefore, our "repurposing old aptamers for new uses" strategy and its integrated computational methods are fast and rational for the discovery of high-affinity aptamers and their optimization.

In summary, this study presents a repurposing method for the discovery of high-affinity aptamers, and has successfully developed new DNA aptamers for TTX from the old, thermally stable aptamers. So, our study not only provides potential recognition molecules for the developments of TTX detection technology, but also demonstrates a very promising rational approach to the discovery of high-affinity aptamers.

CRediT authorship contribution statement

Yuanyuan Li: Investigation, Methodology, Formal analysis, Visualization, Writing – original draft, Writing – review & editing. **Menghua Song:** Formal analysis, Visualization, Writing – original draft. **Ruihua Gao:** Investigation, Formal analysis. **Feng Lu:** Conceptualization, Formal analysis, Funding acquisition. **Jianping Liu:** Supervision, Conceptualization, Formal analysis. **Qiang Huang:** Supervision, Conceptualization, Formal analysis, Writing – original draft, Writing – review & editing, Funding acquisition.

Declaration of Competing Interest

The authors declare that they have no known competing financial interests or personal relationships that could have appeared to influence the work reported in this paper.

Acknowledgments

This work was supported by the National Major Scientific and Technological Special Project for "Significant New Drugs Development" [No. 2018ZX09J18112], the Natural Science Foundation of China [No. 31971377, 31671386], the National Key Research and Development Program of China [No. 2021YFA0910604], and the Shanghai Municipal Science and Technology Major Project [2018SHZDZX01] and ZJLab.

Appendix A. Supplementary data

Supplementary data to this article can be found online at https://doi.org/10.1016/j.csbj.2022.04.033.

References

[1] Bane V, Lehane M, Dikshit M, et al. Tetrodotoxin: chemistry, toxicity, source, distribution and detection. Toxins 2014;6:693–755.
[2] Saoudi M, Abdelmouleh A, El Feki A. Tetrodotoxin: a potent marine toxin. Toxin Rev 2010;29:60–70.
[3] Makarova M, Rycek L, Hajicek J, et al. Tetrodotoxin: history, biology, and synthesis. Angew Chem Int Ed 2019;58:18338–87.
[4] Saoudi M, Ben Rabeh F, Jammoussi K, et al. Biochemical and physiological responses in Wistar rat after administration of puffer fish (Lagocephalus lagocephalus) flesh. J Food Agric Environ 2007;5:107–11.
[5] Noguchi T, Ebesu JSM. Puffer poisoning: epidemiology and treatment. J Toxicol-Toxin Rev 2001;20:1–10.
[6] Guardone L, Maneschi A, Meucci V, et al. A global retrospective study on human cases of tetrodotoxin (TTX) poisoning after seafood consumption. Food Rev Int 2020;36:645–67.
[7] How CK, Chern CH, Huang YC, et al. Tetrodotoxin poisoning. Am J Emerg Med 2003;21:51–4.
[8] Madejska A, Michalski M, Osek J. Marine tetrodotoxin as a risk for human health. J Vet Res 2019;63:579–86.
[9] Vilarino N, Louzao MC, Vieytes MR, et al. Biological methods for marine toxin detection. Anal Bioanal Chem 2010;397:1673–81.
[10] Gerssen A, Mulder PPJ, McElhinney MA, et al. Liquid chromatography-tandem mass spectrometry method for the detection of marine lipophilic toxins under alkaline conditions. J Chromatogr A 2009;1216:1421–30.
[11] Leonardo S, Kiparissis S, Rambla-Alegre M, et al. Detection of tetrodotoxins in juvenile pufferfish Lagocephalus sceleratus (Gmelin, 1789) from the North Aegean Sea (Greece) by an electrochemical magnetic bead-based immunosensing tool. Food Chem 2019;290:255–62.
[12] Wang ZJ, Chen ENN, Yang G, et al. Research advances of aptamers selection for small molecule targets. Chinese J Anal Chem 2020;48:573–82.
[13] Radom F, Jurek PM, Mazurek MP, et al. Aptamers: molecules of great potential. Biotechnol Adv 2013;31:1260–74.
[14] Kim YS, Gu MB. Advances in aptamer screening and small molecule aptasensors. Adv Biochem Eng Biot 2014;140:29–67.
[15] Ye W, Liu TM, Zhang WM, et al. Marine toxins detection by biosensors based on aptamers. Toxins 2020;12:878–904.
[16] Robertson DL, Joyce GF. Selection *in vitro* of an RNA enzyme that specifically cleaves single-stranded DNA. Nature 1990;344:467–8.
[17] Ellington AD, Szostak JW. Selection *in vitro* of single-stranded DNA molecules that fold into specific ligand-binding structures. Nature 1992;355:850–2.
[18] Morris KN, Jensen KB, Julin CM, et al. High affinity ligands from *in vitro* selection: complex targets. Proc Natl Acad Sci USA 1998;95:2902–7.
[19] Ellington AD, Szostak JW. *In vitro* selection of RNA molecules that bind specific ligands. Nature 1990;346:818–22.
[20] Mendonsa SD, Bowser MT. *In vitro* selection of high-affinity DNA ligands for human IgE using capillary electrophoresis. Anal Chem 2004;76:5387–92.
[21] Keefe AD, Pai S, Ellington A. Aptamers as therapeutics. Nat Rev Drug Discov 2010;9:537–50.
[22] Sun H, Zu Y. A highlight of recent advances in aptamer technology and its application. Molecules 2015;20:11959–80.
[23] Nimjee SM, Rusconi CP, Sullenger BA. Aptamers: an emerging class of therapeutics. Annu Rev Med 2005;56:555–83.
[24] Guan BZ, Zhang XW. Aptamers as versatile ligands for biomedical and pharmaceutical applications. Int J Nanomed 2020;15:1059–71.
[25] He F, Wen NC, Xiao DP, et al. Aptamer-based targeted drug delivery systems: current potential and challenges. Curr Med Chem 2020;27:2189–219.
[26] Duan N, Wu SJ, Dai SL, et al. Advances in aptasensors for the detection of food contaminants. Analyst 2016;141:3942–61.
[27] Yu HX, Alkhamis O, Canoura J, et al. Advances and challenges in small-molecule DNA aptamer isolation, characterization, and sensor development. Angew Chem Int Ed 2021;133:2–26.
[28] Berezovski M, Musheev M, Drabovich A, et al. Non-SELEX selection of aptamers. J Am Chem Soc 2006;128:1410–1.
[29] Bunka DHJ, Stockley PG. Aptamers come of age - at last. Nat Rev Microbiol 2006;4:588–96.
[30] Shen H, Li Z, Jiang Y, et al. Structural basis for the modulation of voltage-gated sodium channels by animal toxins. Science 2018;362:eaau2596.
[31] Reuter JS, Mathews DH. RNAstructure: software for RNA secondary structure prediction and analysis. BMC Bioinform 2010;11:129.
[32] Yesselman JD, Das R. Modeling small noncanonical RNA motifs with the rosetta FARFAR server. Methods Mol Biol 2016;1490:187–98.
[33] Ahmad NA, Zulkifli RM, Hussin H, et al. *In silico* approach for post-SELEX DNA aptamers: a mini-review. J Mol Graph Model 2021;105:107872.
[34] Yang L, Ni HJ, Li CL, et al. Development of a highly specific chemiluminescence aptasensor for sulfamethazine detection in milk based on *in vitro* selected aptamers. Sens Actuat B-Chem 2019;281:801–11.
[35] Liu Q, Herrmann A, Huang Q. Surface binding energy landscapes affect phosphodiesterase isoform-specific inhibitor selectivity. Comput Struct Biotechnol J 2019;17:101–9.
[36] Song M, Li G, Zhang Q, et al. *De novo* post-SELEX optimization of a G-quadruplex DNA aptamer binding to marine toxin gonyautoxin 1/4. Comput Struct Biotechnol J 2020;18:3425–33.
[37] Zhu HX, Du WH, Song MH, et al. Spontaneous binding of potential COVID-19 drugs (Camostat and Nafamostat) to human serine protease TMPRSS2. Comput Struct Biotechnol J 2021;19:467–76.
[38] Hou X, Du J, Zhang J, et al. How to improve docking accuracy of AutoDock4.2: a case study using different electrostatic potentials. J Chem Inf Model 2013;53:188–200.
[39] Bitencourt-Ferreira G, Pintro VO, de Azevedo Jr. WF. Docking with AutoDock4. Methods Mol Biol 2019;2053:125–48.
[40] Morris GM, Huey R, Lindstrom W, et al. AutoDock4 and AutoDockTools4: automated docking with selective receptor flexibility. J Comput Chem 2009;30:2785–91.
[41] Huey R, Morris GM, Olson AJ, et al. A semiempirical free energy force field with charge-based desolvation. J Comput Chem 2007;28:1145–52.
[42] A M J A, D T M, C R S B, et al. GROMACS: high performance molecular simulations through multi-level parallelism from laptops to supercomputers. Softwarex 2015;1:19-25.
[43] Wang J, Wolf RM, Caldwell JW, et al. Development and testing of a general amber force field. J Comput Chem 2004;25:1157–74.
[44] Wang J, Wang W, Kollman PA, et al. Automatic atom type and bond type perception in molecular mechanical calculations. J Mol Graph Model 2006;25:247–60.
[45] Sousa da Silva A W, Vranken W F. ACPYPE - AnteChamber PYthon Parser interfacE. BMC Res Notes 2012;5:367.
[46] Darden T, York D, Pedersen L. Particle mesh ewald - an $N\cdot\log(N)$ method for ewald sums in large systems. J Chem Phys 1993;98:10089–92.
[47] Hess B, Bekker H, Berendsen HJC, et al. LINCS: a linear constraint solver for molecular simulations. J Comput Chem 1997;18:1463–72.
[48] Berendsen HJC, Postma JPM, Vangunsteren WF, et al. Molecular-dynamics with coupling to an external bath. J Chem Phys 1984;81:3684–90.
[49] Bussi G, Donadio D, Parrinello M. Canonical sampling through velocity rescaling. J Chem Phys 2007;126:014101.
[50] Jerabek-Willemsen M, Wienken CJ, Braun D, et al. Molecular interaction studies using microscale thermophoresis. Assay Drug Dev Technol 2011;9:342–53.
[51] Cheng S, Zheng B, Yao DB, et al. Study of the binding way between saxitoxin and its aptamer and a fluorescent aptasensor for detection of saxitoxin. Spectrochim Acta A Mol Biomol Spectrosc 2018;204:180–7.
[52] Hirao I, Kimoto M, Lee KH. DNA aptamer generation by ExSELEX using genetic alphabet expansion with a mini-hairpin DNA stabilization method. Biochimie 2018;145:15–21.
[53] Sharma A, Gautam S, Kumar S. Phycotoxins. Food Microbiol 2014;2:25–9.
[54] Huang C-J, Lin H-I, Shiesh S-C, et al. Integrated microfluidic system for rapid screening of CRP aptamers utilizing systematic evolution of ligands by exponential enrichment (SELEX). Biosens Bioelectron 2010;25:1761–6.
[55] Gu H, Duan N, Xia Y, et al. Magnetic separation-based multiple SELEX for effectively selecting aptamers against saxitoxin, domoic acid, and tetrodotoxin. J Agric Food Chem 2018;66:9801–9.
[56] Farokhzad OC, Cheng JJ, Teply BA, et al. Targeted nanoparticle-aptamer bioconjugates for cancer chemotherapy in vivo. Proc Natl Acad Sci USA 2006;103:6315–20.